Rate of CO 2 Attack on Hydrated Class H Well Cement under Geologic Sequestration Conditions

5 AUTHORS, INCLUDING:

Brian R. Strazisar

RJ Lee Group, Inc

57 PUBLICATIONS **1,459** CITATIONS

SEE PROFILE

Gregory V Lowry

Carnegie Mellon University

172 PUBLICATIONS **8,929** CITATIONS

SEE PROFILE

David A. Dzombak

Carnegie Mellon University

200 PUBLICATIONS **5,281** CITATIONS

SEE PROFILE

Rate of CO$_2$ Attack on Hydrated Class H Well Cement under Geologic Sequestration Conditions

BARBARA G. KUTCHKO,[†,‡]
BRIAN R. STRAZISAR,[*,†]
GREGORY V. LOWRY,[‡]
DAVID A. DZOMBAK,[‡] AND
NIELS THAULOW[§]

U.S. Department of Energy, National Energy Technology Laboratory, Pittsburgh, Pennsylvania 15236, Department of Civil and Environmental Engineering, Carnegie Mellon University, Pittsburgh, Pennsylvania 15213, and RJ Lee Group, Inc., Monroeville, Pennsylvania 15146

Experiments were conducted to study the degradation of hardened cement paste due to exposure to CO$_2$ and brine under geologic sequestration conditions (T = 50 °C and 30.3 MPa). The goal was to determine the rate of reaction of hydrated cement exposed to supercritical CO$_2$ and to CO$_2$-saturated brine to assess the potential impact of degradation in existing wells on CO$_2$ storage integrity. Two different forms of chemical alteration were observed. The supercritical CO$_2$ alteration of cement was similar in process to cement in contact with atmospheric CO$_2$ (ordinary carbonation), while alteration of cement exposed to CO$_2$-saturated brine was typical of acid attack on cement. Extrapolation of the hydrated cement alteration rate measured for 1 year indicates a penetration depth range of 1.00 ± 0.07 mm for the CO$_2$-saturated brine and 1.68 ± 0.24 mm for the supercritical CO$_2$ after 30 years. These penetration depths are consistent with observations of field samples from an enhanced oil recovery site after 30 years of exposure to CO$_2$-saturated brine under similar temperature and pressure conditions. These results suggest that significant degradation due to matrix diffusion of CO$_2$ in intact Class H neat hydrated cement is unlikely on time scales of decades.
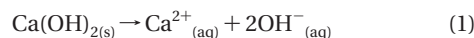
Introduction

The sequestration of CO$_2$ in deep (>1000 m) geologic formations requires a thorough evaluation of potential leakage through any wellbores which penetrate them. It has been proposed that leakage rates of less than 1% of stored CO$_2$ per 100 years are necessary for geologic sequestration to be viable (*1*). An experimental program was established to determine the effects of supercritical CO$_2$ and CO$_2$-saturated brine exposure on wellbore cement at pressure and temperature representative of geologic sequestration conditions. Previous work assessed the effect of curing temperature and pressure on the alteration of Class H neat cement exposed to CO$_2$-saturated brine with the development

of a conceptual model of the degradation process. These previous studies were limited to a CO$_2$ exposure time of 9 days (*2*).
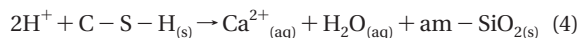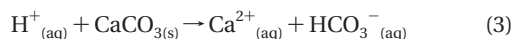
Class H cement is an Ordinary Portland cement (OPC) with a typical Blaine fineness of 1600 cm^2/g. The typical compounds of a Class H cement are 50% tricalcium silicate (Ca$_3$SiO$_5$), 30% dicalcium silicate (Ca$_2$SiO$_4$), 5% tricalcium aluminate (Ca$_3$Al$_2$O$_6$), and 12% tetracalcium aluminoferrite (Ca$_4$Al$_2$Fe$_2$O$_{10}$) (*3*). When the compounds of Portland cement are mixed with water, they form two primary hydration products: calcium-silicate-hydrate (C–S–H) and calcium hydroxide (Ca(OH)$_{2(s)}$). C–S–H is a semi-amorphous, gel-like material that comprises approximately 70 wt% of the hydrated cement and is the principal binding material. (Note: C–S–H is cement industry nomenclature for the nonstoichiometric solid calcium silicate hydrate, not to be confused with a standard chemical formula.) Ca(OH)$_{2(s)}$ is crystalline and comprises roughly 15% to 20% of the hydrated cement. The average CaO/SiO$_2$ ratio of the C–S–H is about 1.7 (*4*).

Two exposure conditions are likely for wellbore cement in a CO$_2$ storage reservoir. Once CO$_2$ is injected, some will remain as a separate free phase (hydrodynamic trapping), while some will dissolve in the brine (solubility trapping) (*5, 6*). Hydrodynamic trapping occurs because the density of the CO$_2$ is less than that of the brine, even at depths of ≥800 m where CO$_2$ is a supercritical fluid. Buoyancy causes the CO$_2$ to rise and spread laterally beneath the reservoir caprock, leading to cement/supercritical-CO$_2$ contact. When the supercritical CO$_2$ contacts formation water it eventually dissolves to form a CO$_2$-saturated brine with pH < 4 (*2*). The dissolved CO$_2$ leads to cement/carbonated brine contact (*6*). This study evaluates cement degradation under these two scenarios, i.e. hydrated cement in contact with CO$_2$-saturated brine and in contact with supercritical CO$_2$.

Previous experiments focused on understanding the chemical dynamics of hydrated Class H neat cement alteration upon initial exposure to CO$_2$-saturated brine and how the cement curing temperature and pressure influenced that alteration. The neat cement was altered by exposure to dissolved CO$_2$-saturated brine at 50 °C and 30.3 MPa. The results of this study involving 9-day exposure suggested that the extent of alteration for longer term exposures may be limited (*2*). The experiments were conducted using a cylindrical cement core inside a high-pressure vessel with the bottom half-submersed in dissolved CO$_2$-saturated brine and the top half-exposed to supercritical CO$_2$ gas. Upon exposure to the CO$_2$-saturated solution, the hardened cement formed well-defined reaction zones in a 2-step process (Figure 1). The first step was the dissolution of Ca(OH)$_{2(s)}$ (Zone 1) and subsequent precipitation of CaCO$_{3(s)}$ (Zone 2).

$$Ca(OH)_{2(s)} \rightarrow Ca^{2+}_{(aq)} + 2OH^-_{(aq)} \qquad (1)$$

$$Ca^{2+}_{(aq)} + HCO_3^-_{(aq)} + OH^-_{(aq)} \rightarrow CaCO_{3(s)} + H_2O \qquad (2)$$

The formation of CaCO$_{3(s)}$ decreases cement permeability and increases its compressive strength (*7*). The second step initiated with the dissolution of CaCO$_{3(s)}$ resulting in leaching of calcium ions from the cement matrix. Without the CaCO$_{3(s)}$, the hardened cement paste no longer has the ability to buffer the pH so the remaining calcium silicate hydrate (C–S–H) is converted to amorphous silica gel.

$$H^+_{(aq)} + CaCO_{3(s)} \rightarrow Ca^{2+}_{(aq)} + HCO_3^-_{(aq)} \qquad (3)$$

$$2H^+ + C-S-H_{(s)} \rightarrow Ca^{2+}_{(aq)} + H_2O_{(aq)} + am-SiO_{2(s)} \qquad (4)$$

* Corresponding author phone: 412-386-5988; fax: 412-386-4806; e-mail: Brian.Strazisar@netl.doe.gov.
† U.S. Department of Energy.
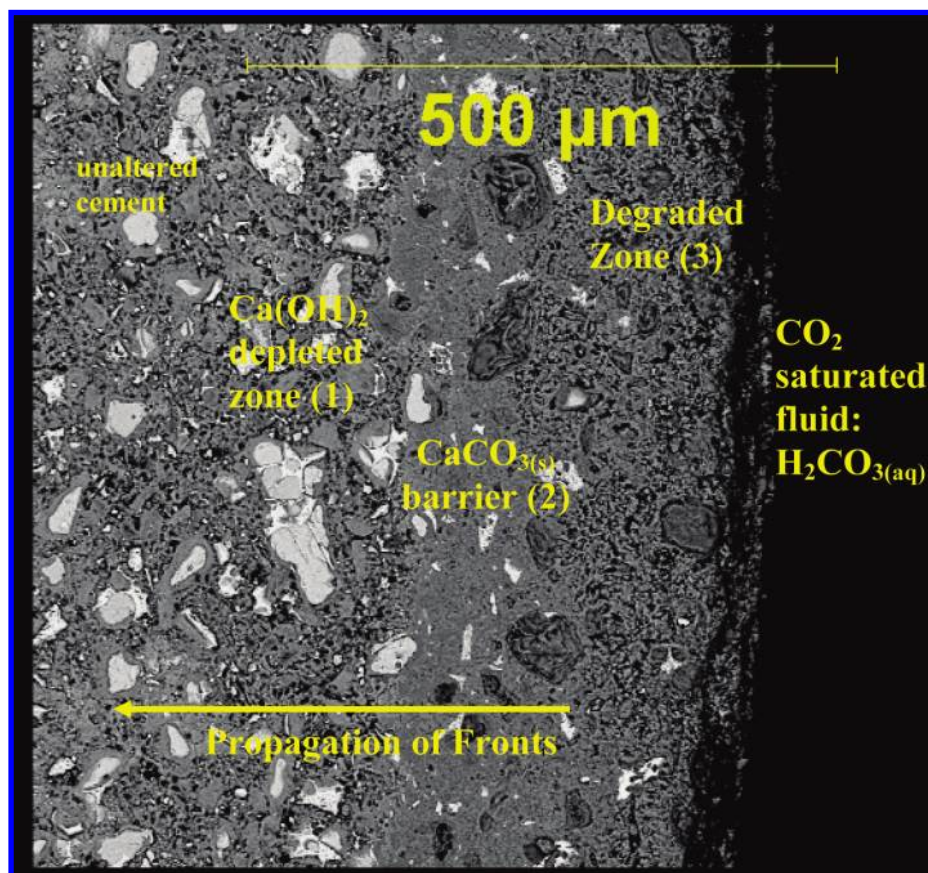‡ Carnegie Mellon University.
§ RJ Lee Group, Inc.

FIGURE 1. SEM-BSE image of Class H neat cement cured for 28 days at 50 °C and 30.3 MPa and exposed for 9 days to CO₂-saturated brine under the same conditions shows the formation of three distinct zones in the cement.

The resulting cement paste of amorphous $SiO_{2(s)}$ has a significant increase in porosity and lacks structural integrity (Zone 3) (2).

The objectives of this research were to investigate the effects of long-term exposure (1 year) of hydrated Class H neat cement to CO_2 under geologic sequestration conditions and specifically to determine the rate of cement degradation that occurs upon exposure to either dissolved CO_2-saturated brine or supercritical CO_2. Extrapolated rates for cement alteration due to long-term exposure to CO_2-saturated brine or supercritical CO_2 were developed and compared with observations of wellbore cements in enhanced oil recovery (EOR) sites where exposure times are ∼30 years. The implications of the projected long-term wellbore cement degradation for geologic sequestration as a viable carbon storage method are discussed.

Experimental Procedures

Class H neat cement samples were mixed according to American Petroleum Institute (API) Recommended Practice 10B (8) (water/cement = 0.38) and cast in cylindrical molds. The samples were submerged in a 1% NaCl (brine) solution in a high pressure vessel at a temperature of 50 °C and water pressure of 30.3 MPa, demolded after 3 days, and allowed to hydrate for a total of 28 days as previously described (2). The curing procedure simulates oil well cement having been placed and cured in the annulus of a well in contact with a saline aquifer.

After the curing period, the hardened cement samples were partially submerged in a 1% NaCl solution, and the vessel was pressurized to 30.3 MPa with CO_2. Total concentration of CO_2 in the brine at these conditions was calculated to be 1.8 M, and the intial pH was calculated to be approximately 2.9 (2). In the high-pressure vessels, the headspace contains supercritical CO_2 and mimics cement exposure to the supercritical phase of the injected CO_2, whereas the submerged (aqueous) phase mimics exposure to the CO_2-saturated brine. The volume ratio of brine to cement was large enough to ensure constant CO_2 concentrations at the solid/water interface for the duration of the experiments (∼87%). The CO_2 experiments were carried out under static conditions (no flow) to simulate downhole/formation conditions (7). A total of 6 samples were placed in a single high-pressure and temperature controlled vessel. Samples were sequentially removed at various intervals up to 1 year. To remove each sample, the pressure was released slowly over a period of 6 h or more to prevent sample damage. No fracturing of the samples was observed as a result of depressurizing.

The cement samples were sectioned and polished in preparation for scanning electron microscope (SEM) analysis. The depth of the altered zones within each cement sample was measured using SEM as previously described and plotted against exposure time (2). Alteration depths were measured on each sample by taking multiple (10 to 15) measurements around the perimeter of a polished section. The penetration depth of each sample was defined as the deepest point that showed evidence of CO_2 reaction. The error bars in the tables and graphs within this manuscript and in the Supporting Information refer to the standard deviation of multiple measurements on a single sample.

Samples were analyzed using an SEM equipped with backscattered electron imaging (BSE) and energy dispersive spectroscopy (EDS). Cement phases were identified using X-ray diffraction (XRD) as described in ref 2.
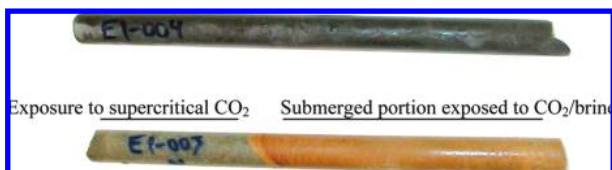
FIGURE 2. Original cement (top) and cement exposed to CO_2 (bottom) after 9 days. The cement exposed to CO_2-saturated brine appears orange in color. This appearance is typical of all exposure times.

Results

Obvious differences were observed between the submerged (CO_2-saturated brine) and headspace (supercritical CO_2) exposed portions of the cement samples upon their removal from the vessels. The outer surface of the submerged cement exposed to the CO_2-saturated brine was orange and had a smooth texture. The portion of cement exposed to the headspace (supercritical CO_2) appeared light gray in color and had a rough texture (Figure 2). SEM analysis of the portion of cement exposed to CO_2-saturated brine revealed 3 distinct zones as previously described (2) (Figure 1). However, these zones were not observed in the headspace samples exposed to supercritical CO_2 indicating a different mode of attack (Figure 3). The cement exposed to supercritical CO_2 had a single reaction front and $CaCO_{3(s)}$ was distributed throughout the reacted portion rather than isolated in a well defined band. $CaCO_{3(s)}$ deposits were also observed on the outside surface accounting for the rough texture. Some supercritical CO_2-exposed samples contained large porous intrusions that deviated significantly from the typical uniform pattern of reaction. The intrusions were only seen in some of the samples and appeared to be random and spatially isolated. These were likely artifacts from condensed droplets of surface moisture on the outer surface of the cement sample and were not included in the measurements to determine penetration depth.

In the CO_2-saturated-brine exposed samples there was an initial rapid rate of alteration depth due to reaction of cement with CO_2 followed by a decrease in rate (Figure 4a–b). With the exception of the intrusions, the cement exposed to supercritical CO_2 showed a more limited penetration and more uniform progression of a carbonated zone (Figure 4a). In all cases the degradation of the cement exposed to supercritical CO_2 was not as deep as that exposed to CO_2-saturated brine. No cement samples were altered beyond a depth of 1 mm after 1 year of exposure.

Discussion

CO_2-Saturated-Brine Exposure. The rate of cement carbonation is diffusion limited (4, 7, 9) because the rate of acid–base carbonation reactions is much faster than the diffusion of ionic species in the cement matrix (9). By definition, ordinary carbonation is the dissolution of CO_2 in the cement pore solution of the cement paste, the production of CO_3^{2-} ions, and the subsequent reaction with Ca^{2+} in order to produce $CaCO_{3(s)}$ within the pore structure of the paste (4). Application of Fick's second law of diffusion with a constant concentration boundary condition is often used to estimate the depth of ordinary carbonation in cement

$$L = \alpha t^{1/2} \qquad (5)$$

where L = depth of carbonation, t = time of exposure, and α is a constant related to the rate of diffusion of ionic species through the cement matrix and depends on the cement permeability, porosity, tortuosity, and chemical composition. A plot of L vs $t^{1/2}$ is linear if Fickian diffusion controls the rate of carbonation (Figure 4a). For exposure to CO_2-saturated

TABLE 1. Extrapolation of Cement Penetration Depths from Ref 15 Compared with Extrapolated Results of this Study

	projected penetration depths (mm)			
	Barlet-Gouédard et al. (16)[a]		Kutchko et al. (present data)[b]	
exposure (years)	supercritical CO_2[c]	CO_2-saturated water[d]	supercritical CO_2[e]	CO_2-saturated brine (0.17 m)[f]
20	110	90	1.37 ± 0.19	0.96 ± 0.06
30	134	112	1.68 ± 0.24	1.00 ± 0.07
50	174	144	2.17 ± 0.31	1.04 ± 0.08

[a] 20 year fit by Barlet-Gouédard et al. (16); 30 and 50 year fit using fitting parameters from 16. [b] Sample mean ± standard deviation of Monte Carlo simulation runs. [c] T = 90 °C, P = 20.68 MPa; extrapolated using a Fickian diffusion equation. [d] T = 90 °C, P = 20.68 MPa; extrapolated using a Fickian diffusion equation. [e] T = 50 °C, P = 30.3 MPa; extrapolated using a Fickian diffusion equation. [f] T = 50 °C, P = 30.3 MPa; extrapolated using the Elovich equation.

brine a linear plot is not observed, indicating that the cement alteration process under the conditions tested is more complex than simple diffusion. An initial rapid reaction followed by a decrease in rate was observed for carbonation of cement exposed to CO_2-saturated brine over 1 year (Figure 4). The parameter α in eq 5 is therefore not constant, implying that the physical properties of the cement are changing likely due to the precipitation of the dense $CaCO_{3(s)}$ rich layer in Zone 2 (Figure 1). Filling the available pore space with solid $CaCO_{3(s)}$ has created a new, denser (less porous) region within the cement. As this new phase grows faster than it is dissolved (see the Supporting Information Figure S1 and Table S2), slower diffusion rates are observed over time, i.e. α decreases with time.

Because α was not constant, the experimental data were fit using the Elovich equation (10)

$$\frac{dL}{dt} = a \exp(-bL) \qquad (6)$$

where L is the penetration depth (mm) at time t (day) of exposure, and a and b are constants determined from the experimental data. The Elovich equation is an empirical model often used to describe two-step uptake or release kinetics involving a rapid initial step followed by a slower step, e.g. of oxygen chemisorption on resin chars (11), and the adsorption or leaching rate of metal ions from solutions with macroporous resins (12). The equation was used in this study because of the good fit with the data (r^2 = 0.97). Integration of eq 6 yields the relationship of penetration depth and time given in eq 7 for the case of $(ab)^{-1}$ being very small (9), which is typical. This was used to fit the experimental CO_2 penetration data (Figure 4b):

$$L = (1/b)\ln t + (1/b)\ln(ab) \qquad (7)$$

The uncertainty of each data point implies a range of values for the Elovich parameters and hence a range of values for extrapolated penetration depth. To take into account the uncertainty in the data, a series of Monte Carlo simulations (13) was run to determine the range of extrapolated penetration depths associated with the uncertainty in the Elovich parameters fitted to the data. Randomly generated values of the penetration depth were selected for each data point in Figure 4b within the range of values measured for that data point (mean ± one standard deviation). The resulting synthetic data set assembled by Monte Carlo sampling was then fitted with the Elovich equation, and least-squares best-
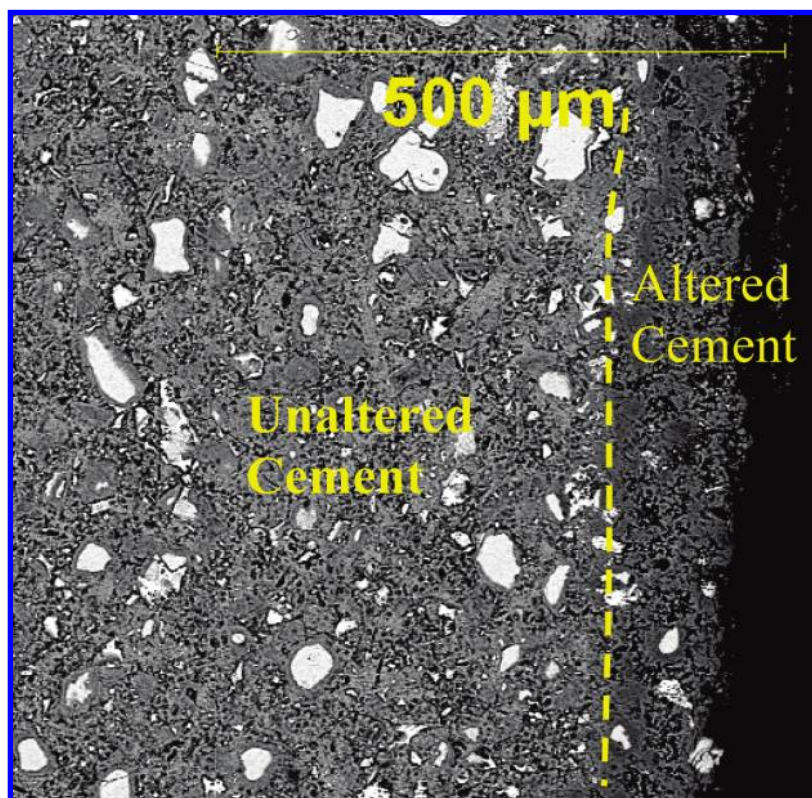
FIGURE 3. SEM-BSE image of Class H neat cement cured for 28 days at 50 °C and 30.3 MPa and exposed for 61 days to supercritical CO_2 under the same conditions shows the formation of a single carbonated zone in the cement. Dashed line approximates boundary of degradation.

fit values of a and b were determined. This was repeated 2000 times. Each set of a and b parameters were substituted back into the Elovich equation to estimate the penetration depth at 20, 30, and 50 years of exposure. The mean and standard deviation of the extrapolated penetration depths from the 2000 simulations are provided in Table 1. Histograms for the extrapolated data are given in Figures S2−S4 of the Supporting Information.

The process observed in the CO_2-saturated brine phase is typical of acid attack, not ordinary carbonation, as documented in the cement solidification/stabilization literature (*14, 15*). Although the specific chemical reactions vary, studies using hydrochloric, nitric, and acetic acid all have yielded similar patterns. Each resulted in the similar scenario of an outer porous zone, an intermediate precipitation zone, and an inner zone leached of calcium hydroxide (*15*). Thus, the scenario observed for cement degradation from exposure to CO_2-saturated brine is best described as an acid attack by carbonic acid.

Supercritical CO_2 Exposure (Headspace)

In contrast to the submerged portion, the cement exposed to supercritical CO_2 (headspace) produced a slow penetration of supercritical CO_2 yielding carbonated paste that did not develop individual distinct alteration zones (Figure 3 and Supporting Information Figure S5). This is likely due to a lack of water to diffuse ions out of the cement matrix. SEM-EDS analysis revealed that the samples underwent ordinary carbonation, where $CaCO_{3(s)}$ precipitates in place and is not as dense. The experimental penetration depths due to supercritical CO_2 exposure exhibited a more linear relationship with respect to the square root of time (Figure 4a). The lack of a dense carbonate barrier allows the reaction to be controlled by the rate of diffusion of CO_2 into the cement matrix and Fickian behavior is assumed for this process (eq

5). Monte Carlo sampling and penetration depth extrapolation simulations (1000) as described above yielded mean penetration depths reported in Table 1 (*13*). Assuming that the long-term rate of alteration continues by the same mechanism observed in the first year, extrapolations predict the extent of penetration from supercritical CO_2 alteration should exceed that of exposure to CO_2-saturated brine within 30 years (Table 1). While the initial rate of penetration of supercritical CO_2 is slower than that of the CO_2-saturated brine due to the absence of water, the rate of penetration is not slowed by the formation of a dense $CaCO_{3(s)}$ layer (as observed for CO_2-saturated brine) and therefore would eventually exceed that of the CO_2-saturated brine case. Histograms for the extrapolated data are indicated in Figures S6−S8 of the Supporting Information.

Comparison of Degradation Rates to Published Laboratory Data and Field Samples

Comparison to existing experimental data in the literature is complicated due to the wide variation in laboratory experimental conditions used in the study of cement degradation. The most similar conditions to our experimental setup are those of Barlet-Gouédard et al. (*16*). Their experiments used static conditions with a Class G cement cured (72 h) and reacted under a pressure of 20.68 MPa (3000 psi) and temperature of 90 °C in pressure vessels similar to our own (*16*). The most significant differences between the conditions of Barlet-Gouédard et al. (*16*) and our own were that they used 1) class G cement rather than Class H cement, 2) a 72 h curing time vs 28 days in this study, 3) an antifoam agent, dispersant, and retarder added to the cement mix to optimize slurry properties vs Class H neat cement in this study, 4) in the use of deionized water, whereas this study used 0.17 M NaCl to simulate brine, and 5) a temperature of 90 °C vs 50 °C used in this study. Extrapolated penetration
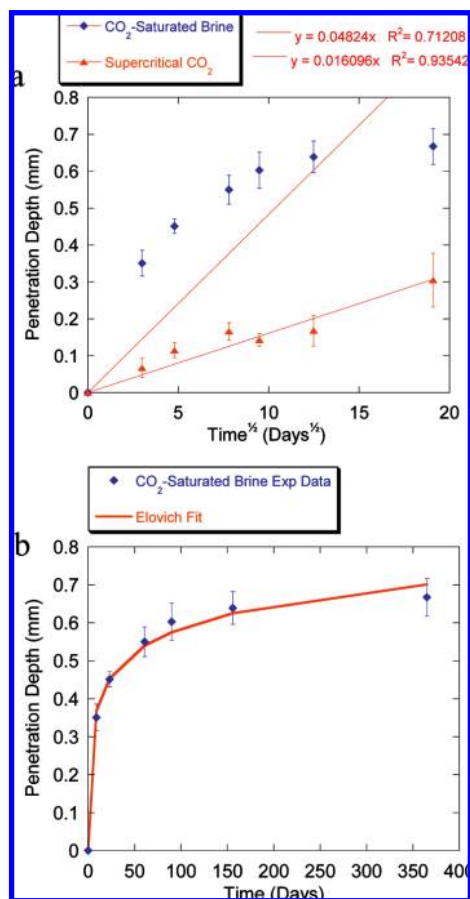
FIGURE 4. Progression of penetration depth for Class H neat cement exposed to CO_2 at 50 °C and 30.3 MPa. Data and sample images are included in the Supporting Information. (a) The CO_2-saturated brine plot is nonlinear with respect to the square root of time indicating non-Fickian behavior. Supercritical phase CO_2 exhibits a more linear plot. (b) Kinetic results for the penetration rate of the CO_2-saturated brine of the cement using the Elovich equation (eq 7; $a = 0.6$, $b = 11.1$).

depths due to exposure to wet supercritical CO_2 and to CO_2-saturated water (15) were calculated using the fitting parameters provided (16) and compared to our supercritical CO_2 and CO_2-saturated brine rates (Table 1).

Both of the Barlet-Gouédard et al. (16) exposure experiments produced alteration zones by a similar degradation process to our CO_2-saturated brine exposure results (2). The longest exposure test was conducted for 3 months. The CO_2 dissolved in water penetration rate followed a diffusion law according to the equation $L = 0.22\ t^{1/2}$ (L in mm, t in h), and the wet supercritical CO_2 followed the equation $L = 0.26t^{1/2}$ (16). The shorter curing time, absence of brine, higher exposure temperature, and possible effects of additives likely account for the significantly higher penetration rates that Barlet-Gouedard et al. (16) observed.

Our laboratory results were also compared to a wellbore cement core recovered from a well at a former enhanced oil recovery (EOR) site (SACROC) (17). The 2130 m deep well was drilled in 1950 and has a shale-limestone reservoir contact at 2000 m. The well was first exposed to CO_2 in 1975, and a total of 120,000 tons of CO_2 have passed through it. For 10 years the well performed as a producer operating under a relatively low pressure environment and later operated as an injector for 7 years subjecting it to a relatively high pressure environment. A sidetrack core was collected from a depth of 1994 m through the well casing and wellbore cement to the shale-limestone reservoir contact at 2000 m. This core
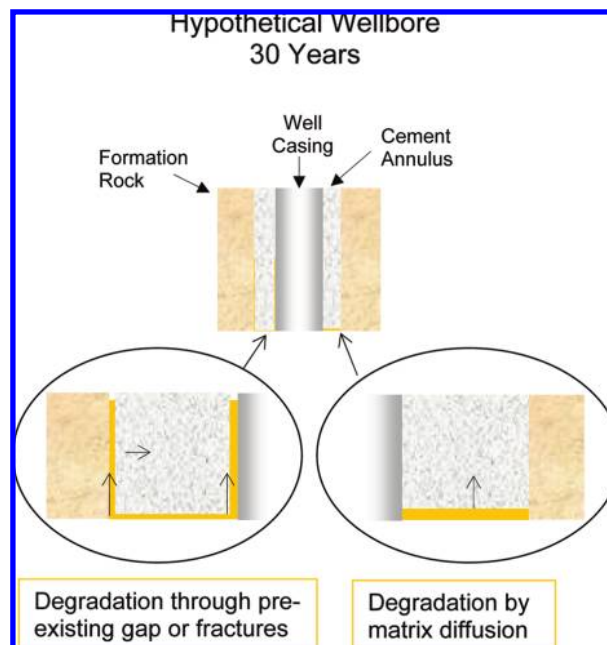

FIGURE 5. Schematic showing degradation by matrix diffusion through intact cement (right) vs CO_2 migration along a pre-existing gaps between the cement-rock and cement-casing interfaces of a hypothetical wellbore.

consisted of the metal casing, the well cement, and a portion of the shale caprock (17).

The SACROC sample was neat cement that likely had been exposed to CO_2-rich brine at approximately 54 °C and 18 MPa for 30 years prior to sampling but maintained structural integrity (17). Carey et al. (17) conclude that CO_2 migrated along a pre-existing gap along the cement-shale interface (between the wellbore and the formation rock). The SACROC cement that had been in contact with the CO_2-rich brine at the cement-shale interface contained the same well-defined altered zones as observed in our CO_2-saturated brine exposed samples. The cement in contact with the CO_2-rich brine at the cement-shale interface had an alteration depth ranging from 1 to 10 mm (17).

In the SACROC cement sample the variability of reaction depth was large (1 to 10 mm) possibly because the interface between the fluid and cement varied in the size of the opening and CO_2 access. Other possibilities which may account for the difference include variations in cement type and water/cement ratio. It is significant that the low end of the observed penetration depth range is comparable to our extrapolated results.

Implications for Cement Integrity under CO_2 Attack

It is highly significant that our laboratory results compared favorably with a wellbore cement core recovered from a well at a former enhanced oil recovery (EOR) site (SACROC). The field sample contained the same well-defined alteration zones as observed in our CO_2-saturated brine exposed samples, and our extrapolated results were in agreement with the low end of the observed penetration depth range of the sample.

The laboratory data and field evidence appear to be consistent and suggest that matrix diffusion in intact cement and subsequent alteration are limited even after 30 years of exposure to CO_2-rich brine. The matrix permeability of a set Class H neat well cement (w/c = 0.38) is extremely low, characteristically in the microdarcy range (3). Based on the alteration process, penetration depths, and rates of alteration observed in this study, and on penetration depths observed in field samples exposed to CO_2 for ~30 years, it is unlikely

that alteration of these cements via cement matrix diffusion of supercritical CO_2 or CO_2-saturated brine would lead to significant alteration in well completions that are properly cemented with Class H neat cement after decades of exposure to supercritical CO_2 or CO_2-rich brine.

The most significant alteration may occur along existing or induced pathways (Figure 5). Existing gaps in the cement-casing and cement-host rock interfaces and fractures within the cement matrix may be widened (by degradation) or sealed (by mineral precipitation) by the cement-CO_2 reactions. Further investigation is required to evaluate the effect of pathways in the cement, geomechanical stress, and of commonly used cement additives.

Acknowledgments

Supporting Information Available

Additional figures and data referenced throughout the text including histograms for the extrapolated data and relevant statistical information. This material is available free of charge via the Internet at http://pubs.acs.org.

Literature Cited

(1) DOE. Carbon Sequestration Technology Roadmap and Program Plan. U.S. Department of Energy: Washington, DC, 2007.
(2) Kutchko, B. G.; Strazisar, B. R.; Dzombak, D. A.; Lowry, G. V.; Thaulow, N. Degradation of Well Cement by CO_2 under Geologic Sequestration Conditions. *Environ. Sci. Technol.* **2007**, *13* (41), 4787–4792.
(3) Nelson, E. B. *Well Cementing*; Schlumberger Educational Services: Sugar Land, TX, 1999.
(4) Taylor, H. F. W. *Cement Chemistry*; Academic Press: New York, 1997.
(5) Bruant, R. G.; Guswa, A. J.; Celia, M. A.; Peters, C. A. Safe Storage of CO_2 in Deep Saline Aquifers. *Environ. Sci. Technol.* **2002**, *36*, 240A–245A.
(6) White, C. M.; Strazisar, B. R.; Granite, E. J.; Hoffman, J. S.; Pennline, H. W. Separation and capture of CO_2 from large stationary sources and sequestration in geological formations–coalbeds and deep saline aquifers. *J. Air Waste Manage. Assoc.* **2003**, *53*, 645–715.
(7) Bruckdorfer, R. A. Carbon dioxide corrosion in oil well cements. SPE 15176, 1986.
(8) API. API Recommended Practice 10B. American Petroleum Institute: Washington, DC, 1997.
(9) Hanečka, K.; Koronthályová, O.; Matiaôvsky, P. The carbonation of autoclaved aerated concrete. *Cem. Concr. Res.* **1997**, *27* (4), 589–599.
(10) Allen, J. A.; Scaife, P. H. The Elovich Equation and Chemisorption Kinetics. *Aust. J. Chem.* **1966**, *19*, 2015–2023.
(11) Teng, H.; Hsieh, C.-T. Activation Energy for Oxygen Chemisorption on Carbon at Low Temperatures. *Ind. Eng. Chem. Res.* **1999**, *38*, 292–297.
(12) Juang, R.-S.; Chen, M.-L. Application of the Elovich Equation to the Kinetics of Metal Sorption with Solvent-Impregnated Resins. *Ind. Eng. Chem. Res.* **1997**, *36*, 813–820.
(13) R Development Core Team. R: A language and environment for statistical computing. R Foundation for Statistical Computing: Vienna, Austria, 2006; ISBN 3-900051-07-0. URL http://www.R-project.org.
(14) Baker, P. G.; Bishop, P. L. Prediction of metal leaching rates from solidified/stabilized wastes using the shrinking unreacted core leaching procedure. *J. Hazard. Mater.* **1997**, *52*, 311–333.
(15) St. John, D. A.;Poole, A. W.; Sims, I. *Concrete Petrography*; Arnold Publishers: London, England, 1998.
(16) Barlet-Gouédard, V.; Rimmelé, G.; Goffé, B.; Porcherie, O. Mitigation strategies for the risk of CO_2 migration through wellbores. IADC/SPE 98924, 2006.
(17) Carey, J. W.; Wigand, M.; Chipera, S. J.; WoldeGabriel, G.; Pawar, R.; Lichtner, P. C.; Wehner, S. C.; Raines, M. A.; Guthrie, G. D. Analysis and performance of oil well cement with 30 years of CO_2 exposure from the SACROC unit, West Texas, USA. *Int. J. Greenhouse Gas Control* **2007**, *1* (1), 75–85.

ES800049R